I&EC research
Industrial & Engineering Chemistry Research

Article

pubs.acs.org/IECR

Boric Acid Production from Colemanite Together with ex Situ CO_2 Sequestration

Mehmet Gönen,*[,†,‡] Emmanuel Nyankson,[‡,§] and Ram B. Gupta[‡]

[†]Department of Chemical Engineering, Engineering Faculty, Süleyman Demirel University, Batı Yerleşkesi, Isparta 32260, Turkey

[‡]Chemical and Life Science Engineering, School of Engineering, Virginia Commonwealth University, Richmond, Virginia 23284-3068, United States

[§]Department of Materials Science and Engineering, University of Ghana, LG 25, Legon-Accra, Ghana

Supporting Information

ABSTRACT: In this work, boric acid (H_3BO_3) production from the mineral colemanite ($Ca_2B_6O_{11}\cdot 5H_2O$) with carbon dioxide (CO_2) sequestration is investigated. CO_2, a known greenhouse gas, is used as a raw material in the leaching of boric acid from colemanite, and the residual calcium is converted into the thermodynamically stable carbonate form. Experiments are carried out in a high pressure stainless steel reactor equipped with stirring and ultrasonic mixing. The solid/liquid ratio is kept at 0.1 g/mL considering the solubility of boric acid extracted, and two different particle sizes (45 and 75 μm) of colemanite are tested. Reactions were carried out for different reaction times and at 40−70 °C and at 4−12 MPa. Characterization of the products by FTIR, XRD, and TGA confirmed that boric acid is extracted from colemanite and CO_2 is converted into calcium carbonate. The conversion favorably increases with the addition of CO_2 pressure up to 8 MPa. The use of 20−25 kHz ultrasound in this heterogeneous reaction increased the extraction efficiency from approximately 70% to 90% due to enhanced mass transfer. CO_2 storage capacity of colemanite is measured as 0.17 as compared to the theoretical value of 0.21 kg CO_2/kg mineral. The utilization of CO_2 in boric acid production can sequester a significant amount of CO_2 while improving the environmental performance as compared to traditional sulfuric acid-based processes.

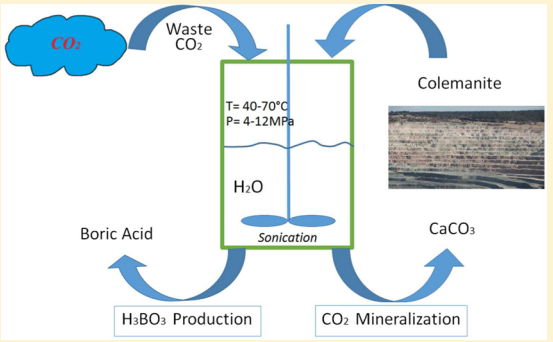

1. INTRODUCTION

The rate of CO_2 emission to the atmosphere has accelerated significantly due to the increasing fossil fuel consumption. The concentration of CO_2 in the atmosphere was 320 ppm in 1960, and it has recently reached a value of 401 ppm in 2015.[1] This level is alarming as the concentration of CO_2 had never exceeded 300 ppm during the past 650 000 years.[2] Annual CO_2 emission to the atmosphere based on human usage is about 13.46 Gtons with the majority from power generation.[3] The CO_2 increase in atmosphere has resulted in global warming, sea level rise, and acidification of oceans.[4] As alternative energy sources such as wind, solar, and biofuels are not likely to fully replace the conventional fossil fuels soon, a recent consensus is that CO_2 emissions from postcombustion must be captured and stored in stable forms to lessen its effects on the earth.

There have been many techniques suggested for CO_2 capture and storage including deep well injection into saline aquifers, ocean injection, underground storage especially into the depleted petroleum reservoirs, and mineralization.[3,5] Out of this mineralization is a reliable method to convert CO_2 into stable compounds. CO_2 mineralization can be carried out in two ways: underground mineralization via reaction with untreated minerals (in situ) and mineralization using physically processed minerals (ex situ). In the first, CO_2 is injected into geological formations where CO_2 and present minerals react to form stable compounds like carbonates. In the latter, minerals are subjected to some unit operations, such as excavation, transportation, size reduction, and sieving. They are then used in the reaction to sequester CO_2. Both techniques have some advantages and disadvantages. For instance, pretreatment of minerals constitutes a major cost in the ex situ process. On the other hand, geological storage has some safety related concerns, for example, the perceived potential for leakage of unreacted CO_2 from the reservoir that may affect nearby people and the environment.

The storage of CO_2 by mineral sequestration or mineral carbonation has been widely studied since 1990, when Seifritz first suggested carbon capture and storage.[6] In fact, CO_2 mineralization is a naturally occurring phenomenon in which dissolved CO_2 in water reacts with, for example, calcium (Ca) and magnesium (Mg) cations among others in rocks to form more stable calcium and magnesium carbonates. The rate-limiting step in that natural carbon storage is the dissolution of

Received: January 26, 2016
Revised: April 12, 2016
Accepted: April 12, 2016
Published: April 12, 2016

DOI: 10.1021/acs.iecr.6b00378
Ind. Eng. Chem. Res. 2016, 55, 5116−5124

CO_2. The rate of reaction between cations and dissolved CO_2 can be increased by increasing the partial pressure of CO_2 and/or by the introduction of some catalysts.

Abundant mineral reserves, such as magnesium silicates (e.g., serpentine, olivine),[5] calcium silicates (e.g., wollastonite),[7] and industrial wastes, e.g., coal fly ash[8] and red gypsum,[9] have been examined for CO_2 mineralization. It was pointed out that two major problems, extraction of active component from minerals and slow reaction rate in CO_2 mineral, must be solved for commercial usage.[10] The use of $Mg(OH)_2$ for indirect CO_2 capture and storage was studied at 80−150 °C to produce magnesite.[11] In order to increase the crystal nucleation and growth, $MgCO_3$ and Al_2O_3 were added to the reaction media as a seed. The minerals that will be used for CO_2 storage must undergo unit operations such as excavation, milling, and sieving, which increases the cost. Mineral processing cost ranges from $15 to $48 per ton of ore, and the cost of CO_2 storage varies from $55 to $250 per ton of CO_2[12] depending on the source of fuel and the type of combustion cycle. As mineral processing cost is high and end products have low commercial value, the CO_2 mineralization technique was excluded from carbon capture and storage (CSS) options by the European Union (EU) CCS Directive.[13] In the EU, geological storage is accepted as the only way of CO_2 storage.[14] Instead of completely excluding the CO_2 mineralization option, the utilization of CO_2 as a raw material for producing high value products using different minerals should be investigated. In this context, CO_2 could be used as a raw material for extracting boric acid from the mineral colemanite and sequestering CO_2 as calcium carbonate during the same process.

Boron exists in the form of borate salts in nature, and most of the boron reserves in the world are located in Turkey. Boric acid (H_3BO_3) is an important boron chemical which is mainly produced from colemanite. Although there are more than 200 boron compounds known in the world, only calcium borates and sodium borates are commercially important and they form about 90% of the existing reserves.[15] Colemanite alone forms 70% of the total Turkish boron reserves. The state owned Eti Maden Inc. in Turkey produces boric acid from the reaction of colemanite and sulfuric acid at 88−92 °C under atmospheric pressure as shown in eq 1.[16] In this process, the use of highly concentrated sulfuric acid causes corrosion problems in the reactor and other units, and spent liquid stored in outdoor ponds poses environmental challenges. Energy requirements of this process, especially in crystallization and drying units, are supplied by coal or natural gas generated power.

$$Ca_2B_6O_{11}\cdot 5H_2O_{(s)} + 2H_2SO_{4(l)} + 6H_2O_{(l)} \rightarrow 2CaSO_4 \cdot 2H_2O_{(s)} + 6H_3BO_{3(aq)} \quad (1)$$

The utilization of CO_2 in boric acid production was suggested by Nies in 1962,[17] where sodium bicarbonate and boric acid were crystallized successively in the solution by varying the temperature (25−75 °C) and CO_2 pressure (2−42 bar). The formation of calcite in boron reserves of Turkey was investigated by bubbling CO_2 gas in the suspension of colemanite and water.[18] The extraction efficiency of boric acid from calcined colemanite increased parallel to the calcination temperature. A boric acid extraction efficiency of 96.3% was obtained from the colemanite which was calcined at 400 °C.[18] Although calcination increases extraction efficiency, it consumes a significant amount of energy; thus, it is not feasible to implement this process on an industrial scale.

The production of boric carbonate and sodium bicarbonate from borax solutions using CO_2 gas was studied recently.[19] The main problem here is in the difficulty in separation of sodium bicarbonate from boric acid as they are both soluble in water. However, if both products could be used together for a specific industry such as ceramic or glass, there would not be any separation step in that process.[19] Instead of borax, the use of colemanite would be a good option as Ca cations could be a good source for CO_2 mineralization.

Ata and co-workers studied the boric acid extraction from colemanite by using CO_2 (3 bar) saturated water. For the optimum conditions, the boric acid extraction efficiency from the colemanite ore and the calcined colemanite was approximately 75% and 99.6%, respectively.[20] The calcination of the mineral does give a good efficiency, but it is not feasible for large scales due to the high energy cost.

Carbon dioxide dissolves in water by forming carbonic acid (eq 2) which further dissociates to produce protons (eq 3) that are utilized in acid leaching of colemanite. The carbonic acid reacts with calcium from the mineral to produce calcium carbonate.

$$CO_{2(g)} + H_2O_{(l)} \leftrightarrow H_2CO_{3(aq)} \quad (2)$$

$$H_2CO_{3(aq)} \leftrightarrow HCO_3^-{}_{(aq)} + H^+{}_{(aq)} \quad (3)$$

$$HCO_3^-{}_{(aq)} \leftrightarrow CO_3^{2-}{}_{(aq)} + H^+{}_{(aq)} \quad (4)$$

The extent and rate of conversion can be further increased by increasing CO_2 pressure. For example, we recently introduced the use of supercritical carbon dioxide.[21] As the reaction takes place in the aqueous medium, the solubility of CO_2 in water is important. Recently, solubility of CO_2 in water was investigated from 0 to 300 °C and from 10 to 120 MPa by using Raman Spectroscopy. Its solubility was reported as 1.06 mol CO_2/kg H_2O at 10 MPa and at 60 °C.[22] Another significant parameter is pH of the solution which is directly proportional to the pressure or the CO_2 dissolved. The pH decreases to the value of 3 at 15.4 MPa and 35 °C.[23]

Heterogeneous reactions are great of importance in both chemical and mining industries as most of the reactants are insoluble in the water phase. The utilization of ultrasonic mixing can have a significant effect on reaction and mass transfer rates as ultrasound decreased the diffusion layer thickness on the solid−liquid interfaces.[24] Production of boric acid from insoluble colemanite by sulfuric acid was enhanced by the use of ultrasound.[25] Also, in general, ultrasound can improve the gas−liquid mass transfer.

The purpose of this study is the indepth investigation of the effects of reaction time, temperature, pressure, and sonication on the reaction between colemanite and high pressure CO_2 in aqueous phase. The effect is studied for both reaction kinetics and product quality.

2. EXPERIMENTAL SECTION

2.1. Materials. Colemanite mineral used in this study was obtained from the American Borate Company, USA. Carbon dioxide, CO_2 (99.9 vol %, Praxair), was used for mineralization experiments at different pressures. Sodium hydroxide, NaOH (99 wt %, Merck), glycerol, $C_3H_8O_3$ (99 wt %, Acros Organics), phenolphthalein ($C_{20}H_{14}O_4$, Merck) and methyl red ($C_{15}H_{15}N_3O_2$, Merck) indicators, sulfuric acid, H_2SO_4 (96 wt %, Merck), and sodium carbonate, Na_2CO_3 (99 wt %,

DOI: 10.1021/acs.iecr.6b00378
Ind. Eng. Chem. Res. 2016, 55, 5116−5124

Merck), were used in the analytical determination of B_2O_3 content of the aqueous phase and initial raw colemanite. The factor value of NaOH solution was determined by using a potassium hydrogen phthalate (KHP; $C_8H_4KO_4$ (99.5 wt %, Merck)), which is not affected by the humidity in air during weighing. Thus, a solution prepared by KHP can be used to determine the precision of the NaOH solution in the titration procedure.

2.2. Raw Material Characterization and Analysis of B_2O_3. B_2O_3 content of colemanite was determined by volumetric methods by dissolving a known amount of colemanite in H_2SO_4 solution (33 vol %). Acidity induced by unreacted H_2SO_4 in the solution was neutralized with Na_2CO_3, and the end point was determined by using 6 M NaOH in the presence of methyl red indicator. Glycerol was then added to the solution, and the acidity induced by boric acid was determined with 0.5 M NaOH in the presence of phenolphthalein indicator.[26]

2.2.1. Colemanite–CO_2 Reaction in Aqueous Phase. Figure 1 shows the experimental setup used for CO_2 mineralization

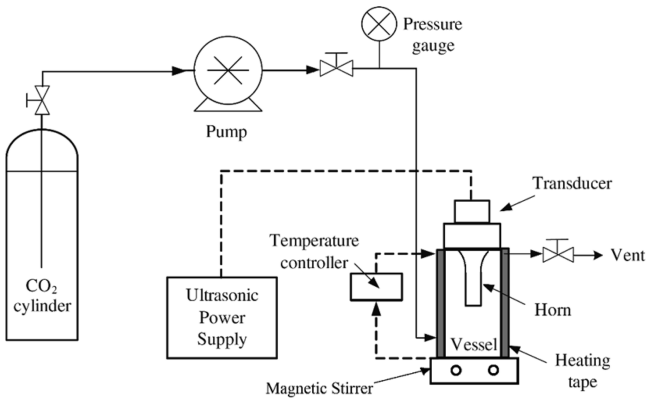

Figure 1. Apparatus for boric acid production from colemanite with CO_2 sequestration.

and boric acid extraction. It consists of a CO_2 gas cylinder with a dip tube, a high pressure pump (Scientific System Inc.) for pumping CO_2, an ultrasonic processor (Columbia International Inc.) producing ultrasonic waves at a frequency of 20–25 kHz with maximum power capability of 1000 W, and a 200 mL stainless steel mixing vessel heated externally by a heating tape. Power of the transducer depends on the resistance to the movement of the horn which is affected by setup and process parameters, e.g., reactor volume, horn size, mixture viscosity, and pressure in the reactor. In the sonication experiment, 50% of maximum power was used for 1.1 s on and 1.1 s off during the experiment. The ultrasonic processor consists of three major components: an ultrasonic power supply, a transducer, and a horn with 10 mm tip diameter. Colemanite samples supplied by American Borate Inc. were used directly in the experiments. An amount of 15.0 g of colemanite having a mean particle size of 45 and 75 μm was placed into the stainless steel reactor. Then, according to the solid–liquid ratio, 0.1 g/mL, deionized water with resistivity of 18.2 MΩ.cm was added to the reactor and its lid was closed. The reactor was pressurized by using a CO_2 pump, and the reactions were carried out under 550 rpm magnetic stirring (Fischer Scientific, Isotemp). The reactor was heated externally, and the temperature was measured internally by the help of thermocouple and temperature controller (Bernant Company R/S Model).

The hydronium ion (H_3O^+) formed when CO_2 dissolves in water (eq 5) attacks the colemanite structure according to the reaction in eq 6, and Ca^{2+} cations are formed. Those cations and carbonate anions react to produce calcium carbonate (eq 7). Apart from those reactions, calcium bicarbonate may also be produced from the reaction of calcium and bicarbonate ions as shown in eq 8.

$$2CO_{2(g)} + 6H_2O_{(l)} \leftrightarrow 4H_3O^+_{(aq)} + 2CO_3^{2-}{}_{(aq)} \quad (5)$$

$$2CaB_3O_4(OH)_3{\cdot}H_2O_{(s)} + 4H_3O^+_{(aq)} \rightarrow 6H_3BO_{3(aq)} + 2Ca^{2+}_{(aq)} + 2H_2O_{(l)} \quad (6)$$

$$2CO_3^{2-}{}_{(aq)} + 2Ca^{2+}_{(aq)} \rightarrow 2CaCO_{3(s)} \quad (7)$$

$$2HCO_3^-{}_{(aq)} + Ca^{2+}_{(aq)} \rightarrow Ca(HCO_3)_{2(aq)} \quad (8)$$

As the CO_2 dissolves in water, carbonic acid is formed, releasing protons (H^+) that attack colemanite to open up its structure. The pH of the water exposed to CO_2 gas at room temperature and 100 kPa is about 4. However, when pressure is increased to 6.23 MPa, pH decreases to 3 at 35 °C.[23] Pressure and temperature ranges for the reaction were determined on the basis of pressure–pH data[23] and critical properties of CO_2.[27] Experimental conditions of the CO_2–colemanite reaction at different experiments are given in Table 1. 15.0 g of colemanite, 0.1 (g/mL) solid–liquid (S/L) ratio, different reaction times, temperature, and different CO_2 pressures were used in the experiments.

Table 1. Experimental Conditions for CO_2–Colemanite Reaction Carried out at a Solid–Liquid Ratio of 0.1 g/mL

exp. no.	temperature, °C	reaction time, min.	pressure, MPa	feed particle size, μm
1	50	30	6	45
2	50	60	6	45
3	50	120	6	45
4	50	180	6	45
5	40	60	6	45
6	60	60	6	45
7	70	60	6	45
8	50	30	8	45
9	50	30	10	45
10	50	30	12	45
11	70	10	6	45
12[a]	70	10	6	45
13[a]	50	30	6	45
14	70	10	6	75
15	50	30	4	45

[a]Sonication was used in these experiments.

All the experiments were carried out in a batch process. After the reaction, the reactor was cooled and depressurized; the slurry was filtered (1–3 μm filter) under vacuum (650 mmHg), and filter cake was washed by hot deionized water. The filter cake was dried in an air-circulation oven at 105 °C until a constant weight was attained. Solid products obtained from filter cake and filtrate were characterized by FTIR, XRD, and TGA. Boric acid content of the liquid phase was determined by analytical titration by 0.5 M NaOH in the presence of glycerol and phenolphthalein indicator.[26]

DOI: 10.1021/acs.iecr.6b00378
Ind. Eng. Chem. Res. 2016, 55, 5116–5124

Table 2. Conversion of Colemanite at Various Experimental Conditions

exp. no.	temperature, °C	reaction time, min.	pressure, MPa	conversion, %	kg CO_2/kg colemanite
1	50	30	6	69.8	0.12
2	50	60	6	85.5	0.14
3	50	120	6	90.5	0.15
4	50	180	6	99.0	0.17
5	40	60	6	73.3	0.12
6	60	60	6	92.7	0.16
7	70	60	6	99.4	0.17
8	50	30	8	71.1	0.12
9	50	30	10	73.2	0.12
10	50	30	12	74.6	0.13
11	70	10	6	73.3	0.12
12[a]	70	10	6	91.2	0.15
13[a]	50	30	6	89.9	0.15
14	70	10	6	71.1	0.12
15	50	30	4	58.4	0.10

[a]Sonication was used in these experiments.

2.2.2. Characterization of Solid Products. Solid products formed (a filter cake and a powder crystallized from the aqueous phase) were examined by X-ray diffraction (XRD), attenuated total reflectance Fourier transform infrared spectroscopy (ATR-FTIR), and thermal gravimetric analysis (TGA). For this purpose, 20 mL of filtrate solution was crystallized by evaporating at 50 °C. The solid white crystals obtained were weighed, and the total amount of powder product was determined from the filtrate volume. X-ray diffractometry (PANanalytical MPD Xpert-Pro) was used to analyze the crystal structures of the colemanite and the formed solid products with Cu Kα radiation at 45 kV and 40 mA. The registrations were performed in the 2θ range of 5−80°. The reflection spectra of powdered samples were obtained using a Fourier transform infrared (FTIR) spectrophotometer (Nicolet Nexus 670 FTIR). A small amount of sample was placed directly on a Smart ATR using a spectrometer and scanned from 4000 to 600 cm^{-1}, averaging 16 scans at 0.482 cm^{-1} data spacing with a resolution of 4 cm^{-1}. Thermal gravimetric analyses (TGA) were performed in Perkin Pyris 1 TGA. Powder samples (5−10 mg) were loaded into an alumina pan and heated from 25 to 900 °C at 10 °C·min^{-1} under N_2 flow (20 mL·min^{-1}).

2.2.3. Analysis of the Filtrate. The liquid phase obtained at the end of the reaction was filtered, and the filtrate was analyzed for B_2O_3 % content by analytical titration three times. At the end of the reaction, B_2O_3 content of aqueous phase and remaining solid byproduct were also determined by using volumetric and gravimetric methods. The results obtained from these calculations are shown in Table 2. Boric acid extraction efficiency was calculated by using the following equation (eq 9):

$$\text{extraction efficiency of } H_3BO_3,\ \% = \left(\frac{M_1}{M_0}\right) \times 100 \tag{9}$$

where M_0 is the amount of boric acid in the colemanite and M_1 is the amount of boric acid dissolved in the aqueous phase.

3. RESULTS AND DISCUSSION

As colemanite is insoluble in water, the reaction of colemanite and CO_2 in aqueous phase is a heterogeneous reaction. While CO_2 dissolves in water, the reaction will proceed to the product side. The rate of CO_2 solubility in water is a significant step which influences the overall reaction rate. In heterogeneous reactions, external mass transfer limitations can be eliminated by either decreasing particle size of solid reactant or increasing mixing rate. In this case, the resistance in the solubility of CO_2 in aqueous phase results in an extra mass transfer limitation. The reaction rate is greatly influenced by the solubility of CO_2 in water and the reaction temperature. The solubility of CO_2 in water is inversely proportional with temperature and directly proportional with pressure. On the other hand, there is competition between reaction rate and gas solubility based on the temperature rise. Another common technique used in heterogeneous reactions is ultrasound, which was studied in this reaction.

The solid−liquid ratio in this reaction was selected as 0.10 g/mL based on boric acid solubility in aqueous phase reported as 4.7 wt % at 20 °C.[28] This ensured that the produced boric acid will be in dissolved form. The parameters considered to be effective in the reaction of colemanite and CO_2 in aqueous phase are reaction temperature, particle size, pressure, and reaction time.

3.1. CO_2 Mineralization via Reaction with Colemanite.

The chemical analysis of the colemanite (by XRF) provided by American Borate Inc. is given in Supporting Information. The sample contains substantial amounts of Si, Mg, Al, and Sr. This result indicates that the colemanite sample contains some impurities in the form of clay, dolomite, strontium borate, and calcite.[16] Pure colemanite consists of B_2O_3 (50.8 wt %) and CaO (27.3 wt %). It was determined that the raw sample contains 79.1 wt % colemanite based on its B_2O_3 content of 40.2 wt %. Although B_2O_3 content of the sample is lower than the theoretical value of colemanite, CaO content of the sample (26.5 wt %) is very close to the theoretical value of colemanite, but this is probably due to some portion of CaO being contributed by impurities such as dolomite.

CO_2 mineralization can be achieved by reacting colemanite and producing boric acid. CO_2 can replace the sulfuric acid used in the current production of boric acid. In addition, CO_2 that is already released from the nearby power generation unit of the boric acid plant can be utilized in the conventional process. Theoretically, colemanite mineral can sequester up to the 214 kg of CO_2 per ton of pure colemanite and 486 kg of $CaCO_3$ is formed. The amount of CO_2 mineralized varies

DOI: 10.1021/acs.iecr.6b00378
Ind. Eng. Chem. Res. 2016, 55, 5116−5124

depending on the purity of the colemanite mineral and its Ca and Mg contents. CO_2 mineralization capacity of colemanite mineral was measured between 0.10 and 0.17 kg CO_2/kg colemanite based on its purity and the extent of conversion (Table 2).

For example, 0.17 kg of CO_2 was sequestered per kg of colemanite in Experiment 7. For comparison, CO_2 mineralization using fly ash was measured as 0.264 kg CO_2/kg fly ash.[8] When the CO_2 capture capacity of colemanite is compared with the other minerals and waste materials, it is seen that colemanite capacity is lower than the others' capacities, but the separation of the boric acid from colemanite is the main advantage for this novel CO_2 mineralization process.

The effect of particle size was investigated in Exp. 11 and Exp. 14 by keeping all other parameters constant. In commercial boric acid production, colemanite with a particle size of <100 μm is used.[29] Thus, ground colemanite (particle size of 45 and 75 μm) was used in this study. The use of colemanite with lower particle size can accelerate the reaction, but it is economically not feasible. When the particle size was increased from 45 to 75 μm, the reaction conversion slightly reduced from 73.3% to 71.1% as expected. As particle size is inversely proportional to the surface area, increasing particle size decreases the surface area and vice versa. The use of 75 μm colemanite in the reaction resulted in a lower conversion value. The deviations in analytical titration experiments caused an error of ±1% in the determination of conversion. On the basis of those deviations, error bars are inserted into the figures related to conversion.

3.2. Characterization. The characterization of the solids that remained in the reactor and crystallized from the liquid was done by X-ray diffraction, infrared spectroscopy, and thermal gravimetric analyses. XRD patterns of those solid samples (Exp. 4) were given in Figure 2. The peaks shown by a star at 2θ

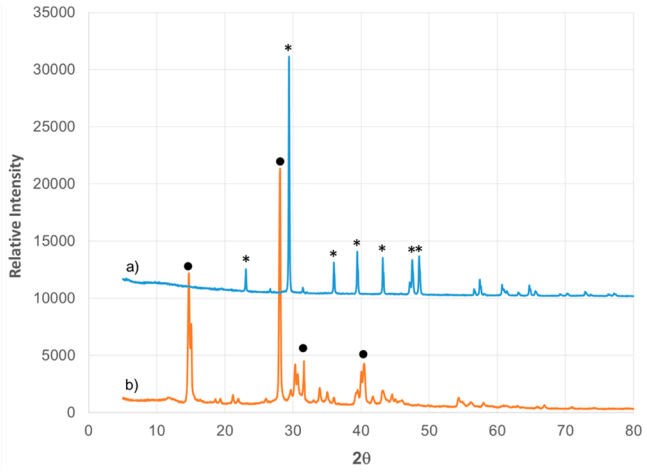

Figure 2. XRD patterns of solids that (a) remained in the reactor and (b) crystallized from the filtrate.

values of 23.1°, 29.4°, 35.9°, 39.4°, 43.2°, 47.5°, and 48.5° on Figure 2a are the characteristic peaks of calcite crystal structure according to the JCPDS:5-0586. The peak with maximum intensity at the 29.4° 2θ value is attributed to the reflections from the (104) plane. The XRD pattern of the powder obtained from crystallization is given in Figure 2b. The peaks represented by full circles at the 2θ value of 14.7° and 28.0° represent the characteristic peak of boric acid as inferred from its crystallographic data (JCPDS 30-0199). The maximum peak at the 2θ value of 28.0° is caused by the reflection from the (002) plane.

Attenuated total reflectance Fourier transform infrared (ATR-FTIR) spectra of the solid that remained in the reactor and the solid crystallized from filtrate are depicted in Figure 3a,b, respectively. The strong carbonate band seen at 871 cm^{-1}

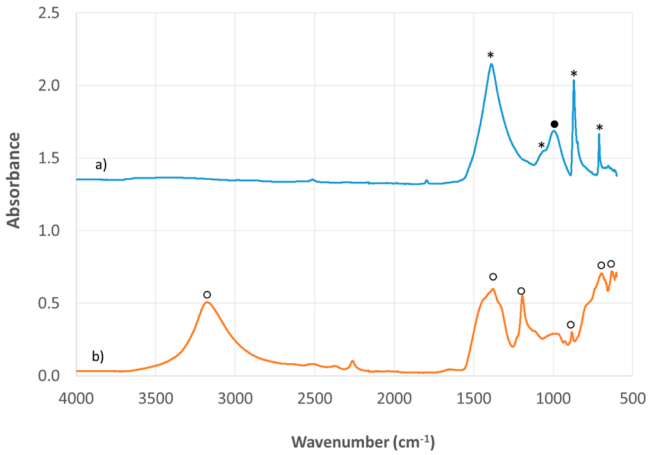

Figure 3. FTIR spectra of solids that (a) remained in the reactor and (b) crystallized from the filtrate.

(out of plane bending, v_2) and the band at 711 cm^{-1} (plane bending) are characteristic vibrations for calcite. On the other hand, the band at 1000 cm^{-1} (shown by the full circle in Figure 3a) is not related to calcite structure but belongs to Si−O and Al−O bonds present in impurity minerals in the sample. The shoulder band observed at 1050 cm^{-1} was assigned to the symmetric stretching vibration and lattice mode vibration. The band at 1390 cm^{-1} is attributed to the out of phase stretching of CO_3 structure which is in the calcite. The vibration modes shown by stars (Figure 3a) are characteristic bands of calcite structure.[30] It must be noted that the band positions in the ATR spectrum may be shifted slightly to the lower wavenumbers as compared with those in the transmission spectrum as a refractive index of the sample interferes in ATR mode. The broad band observed between 2700 and 3500 cm^{-1} wavenumbers on Figure 3b is related to the hydroxyl groups in boric acid structure.[31] The weak band seen at 881 cm^{-1} and strong band at 1374 cm^{-1} wavenumbers are caused by symmetric stretching vibration of B−O and by asymmetric stretching vibration of B−O in the BO_3 structure, respectively. The band observed at 1192 cm^{-1} wavenumber belongs to in-plane bending vibration of the B−O−H structure. Asymmetric and symmetric stretching vibrations of B−O bonding in tetrahedral structure (BO_4) are seen at 1114 and 691 cm^{-1} wavenumbers.[30] From the FTIR spectrum, it was determined that CO_2 leached boric acid from colemanite in the aqueous mixture and the dissolved boric acid was crystallized from solution.

TGA curves of solid samples produced from the reaction of colemanite and CO_2 are shown in Figure 4. A typical thermal behavior of calcite is depicted in Figure 4a. $CaCO_3$ begins to decompose at 600 °C by releasing CO_2, and the total mass loss is 44 wt %.[32] The filter cake obtained in the reaction starts to lose mass at 600 °C and ends at 780 °C with a mass loss of 40 wt %, which is lower than the theoretical or pure $CaCO_3$. The difference in mass losses of theoretical carbonate and filter cake is caused by the impurities present in the raw colemanite

DOI: 10.1021/acs.iecr.6b00378
Ind. Eng. Chem. Res. 2016, 55, 5116−5124

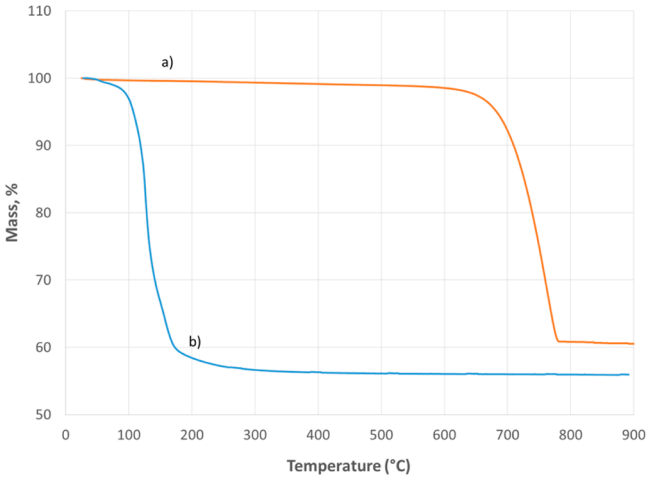

Figure 4. TG curves for solids (a) remaining in the reactor and (b) crystallized from the filtrate.

sample. The crystallized powder from filtrate of Exp. 4 has a mass loss of 43.6 wt % in the temperature range of 60−200 °C (Figure 4b). This thermal behavior is in good agreement with pure boric acid having a mass loss of 43.8 wt %. It was determined that solid formed at the end of the reaction and powder crystallized from filtrate were calcite and boric acid, respectively, as inferred from XRD, FTIR, and TGA analyses.

3.3. Effect of Reaction Time. The effect of reaction time on the dissolution of colemanite by carbonic acid at 6 MPa, 50 °C, and a solid−liquid ratio of 0.1 was investigated between 30 and 180 min as shown in Figure 5. There are two steps in this

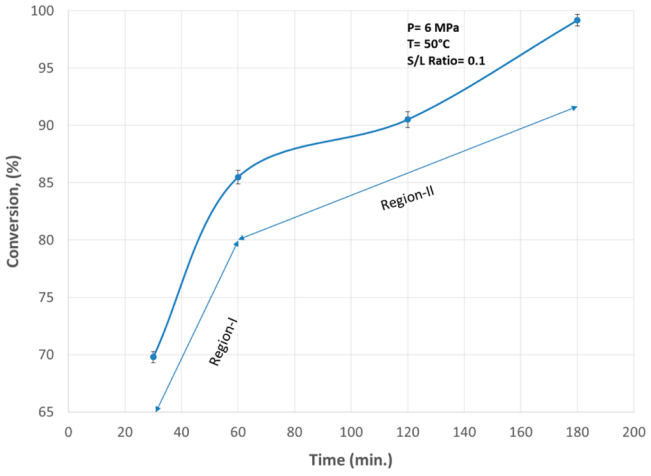

Figure 5. Effect of reaction time on conversion (line is for an eye-guide).

reaction based on the slopes. The first step occurred between 30 and 60 min (Region-I), which is faster than the second step that took place between 60 and 180 min (Region-II). The decrease of the reaction rate with time is related to the amount of mineral consumed during the reaction as inferred from the slope in Region-I being greater than the slope in Region-II. As long as the amount of reactant decreases with time, reaction rate reduces as well. At a 50 °C reaction temperature and 6 MPa pressure, 100% conversion required about 3 h of reaction time. By increasing the reaction temperature, the reaction time can be lowered.

The reaction between colemanite and carbonic acid in aqueous phase is heterogeneous, and the use of CO_2 above its critical points enhances the reaction rate by eliminating mass transfer limitations. The reaction between solid colemanite particles and proton (H^+) released from carbonic acid (H_2CO_3) can be modeled by a shrinking core model,[33] where colemanite particles are assumed to be spherical as shown in Figure 6.

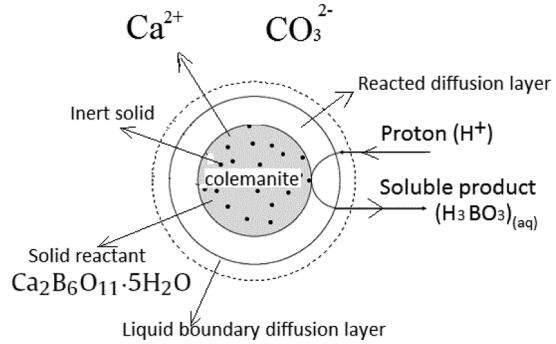

Figure 6. Schematic representation of shrinking core model for colemanite reaction with carbonic acid.

When spherical colemanite particles are digested by carbonic acid, their sizes get smaller (i.e., shrinks). The key steps are as follows:

1. Dissolution of CO_2 in water causes formation of carbonic acid.
2. The carbonic acid dissociates to protons (H^+) and carbonate ions (CO_3^{2-}), and H^+ cations diffuse from the bulk of the liquid through the liquid film to the surface of the solid.
3. Reaction takes place on the solid surface between H^+ and the mineral.
4. Diffusion of dissolved components (Ca^{2+} and H_3BO_3) from the surface of the solid through the liquid film back to the bulk of the liquid phase.
5. Ca^{2+} and CO_3^{2-} react to produce $CaCO_3$ that forms a shell on the mineral surface.

3.4. Effect of Sonication. The mechanical and chemical effects of ultrasound are caused by cavitation bubbles which are generated by sound waves. The mechanical effect is mostly related to the disruption of particles during sonication, and the chemical effect is usually concerned with the formation of highly reactive radicals.[34] The effect of sonication for the colemanite−CO_2−H_2O system was investigated in this study. The use of sonication at 50 °C for 30 min of reaction time increased colemanite conversion from approximately 70% to 90% for the condition given in Figure 7. The same effect was also obtained at 70 °C and for 10 min of reaction time as inferred from Figure 7. As dissolved gases act as nucleation sites for cavitation, the presence of CO_2 dissolved in water under high pressure increases the cavitation. On the other hand, sonication removes the dissolved gases in liquid phase at atmospheric pressure. Although CO_2 is removed from water by sonication, it dissolves again due to high CO_2 pressure in the vessel. The formation of cavitation is helpful for the CO_2−colemanite reaction. There are two significant contributions of sonication in heterogeneous reactions; the first is temperature rise due to power dissipation and the latter is removal of mass transfer resistance on the solid particle surface.[24] The temperature was recorded during the reaction, and it was

DOI: 10.1021/acs.iecr.6b00378
Ind. Eng. Chem. Res. 2016, 55, 5116−5124

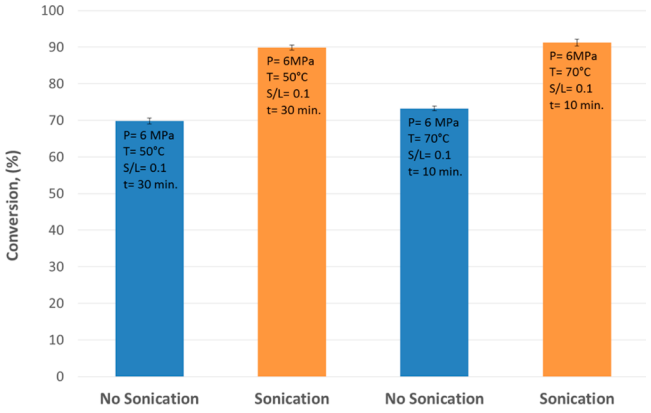

Figure 7. Effect of sonication on the CO_2–colemanite reaction.

found that it tends to increase by 2–7 °C depending on sonication time. As the reaction rate is intensively related to the temperature, the temperature rise due to sonication indirectly helped the reaction rate. Sonication helped also to reduce the byproduct layers (calcite) on the shrinking colemanite particles. In that case, the transfer of H^+ to the particle surface and of Ca^{2+} and H_3BO_3 transfers to the bulk were enhanced. As we did not observe the mineral particle size during the reaction, it is difficult to infer whether the sonication made a significant change or not with regards to decreasing particle size over time.

3.5. Effect of CO_2 Pressure. The effect of pressure was investigated on the reaction of colemanite and CO_2 in aqueous phase. Since the solubility of CO_2 in water is enhanced by pressure, reactions were conducted in the 4–12 MPa pressure range. As it was shown in Figure 8, the conversion increased

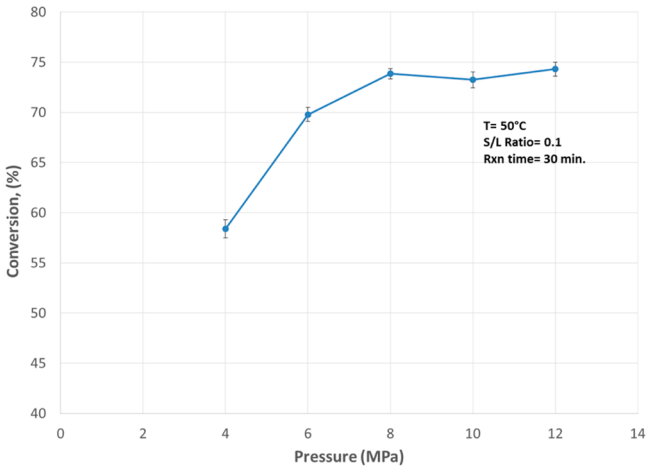

Figure 8. Effect of CO_2 pressure on the reaction.

with rising pressure up to 8 MPa; a further increase of pressure did not make a significant change in conversion. When critical pressure (7.39 MPa) of CO_2 is exceeded, the maximum conversion value is obtained as there is less mass transfer limitation in the supercritical region at the temperatures greater than the critical temperature of CO_2 (31.1 °C). A complete conversion value could be achieved by increasing the reaction time and rising the temperature to the values of 70 °C at 8 MPa pressure. A complete conversion is important since there are difficulties in the separation of powders (unreacted raw material and formed products or byproducts).

The solubility of CO_2 increases sharply with pressure up to 10 MPa at 15 °C as pointed out by Guo and co-workers.[22] After that point, the influence of pressure on CO_2 solubility in water is not as much. This trend generally is seen up to 300 °C. Thus, CO_2 pressure can be applied up to 10 MPa for the colemanite–CO_2 reaction where temperature is lower than 300 °C. The effect of pressure on the colemanite–CO_2 reaction was observed with the same trend of CO_2 solubility in water. As long as the CO_2 dissolves in water, it reacts with colemanite mineral and liberates H_3BO_3 and Ca^{2+}.

3.6. Effect of Reaction Temperature. The effect of temperature (40–70 °C) on the colemanite–CO_2 reaction in aqueous phase was investigated as shown in Figure 9. When

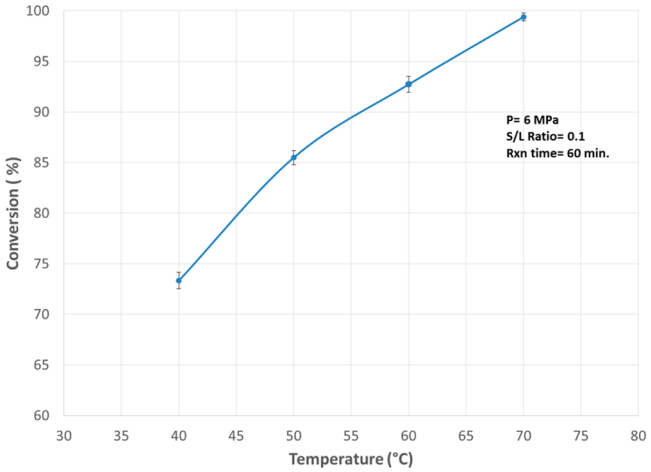

Figure 9. Effect of temperature on the CO_2–colemanite reaction.

temperature is raised from 40 to 70 °C, conversion increased from 73% to 99% at 6 MPa pressure and for 60 min of reaction time (Exp. 5 and Exp. 7). Here, both the reaction temperature (70 °C) and reaction time (1 h) are lower than those in the commercial process which is carried out at 88–92 °C for 3–3.5 h of reaction time.[35] On the basis of the reaction temperature, colemanite–CO_2 reaction consumes less energy overall than the commercial one (colemanite–H_2SO_4). In fact, reaction temperature affects both reaction rate and the solubility of CO_2 in aqueous phase. While the rate of reaction increases with temperature, the solubility of CO_2 decreases with temperature. On the other hand, as the pressure is really high in the reactor, there is equilibrium between CO_2 in aqueous phase and CO_2 in vapor phase. The consumption of CO_2 in the reaction favors the CO_2 dissolution in the aqueous phase. CO_2 solubility in water was reported as 1.06 mol CO_2/ kg H_2O at 10 MPa and 60 °C.[22]

When Exp. 5 and Exp. 11 are compared, the effect of reaction time and temperature can be seen. An increase of reaction temperature from 40 to 70 °C and reduction of reaction time from 60 to 10 min resulted in the same conversion.

4. CONCLUSION

CO_2 can be sequestered while producing boric acid from colemanite. The effects of reaction time, sonication, pressure, and temperature on the CO_2–colemanite reaction are investigated. CO_2 pressure up to 8 MPa improved the carbonation efficiency. When the temperature is raised to 70 °C, the maximum conversion (99.4%) was obtained for 0.1 g/ mL solid–liquid ratio, at 6 MPa and for 60 min. The use of

DOI: 10.1021/acs.iecr.6b00378
Ind. Eng. Chem. Res. 2016, 55, 5116–5124

sonication in this heterogeneous reaction further increased the extraction efficiency from approximately 70% to 90% for 30 min of reaction time by decreasing mass transfer limitations by removing the formed calcite layer on colemanite particles and by decreasing the particle size of colemanite. The best CO_2 mineralization capacity of the reaction with colemanite was 0.17 kg CO_2/kg colemanite. It was determined that the most important parameters in the reaction of colemanite and CO_2 in aqueous phase were temperature and pressure.

■ ASSOCIATED CONTENT

Supporting Information

The Supporting Information is available free of charge on the ACS Publications website at DOI: 10.1021/acs.iecr.6b00378.

Chemical composition of colemanite mineral (PDF)

■ AUTHOR INFORMATION

Corresponding Author

*E-mail: mehmetgonen@sdu.edu.tr.

Notes

The authors declare no competing financial interest.

■ ACKNOWLEDGMENTS

The Scientific and Technical Research Council of Turkey (TÜBİTAK) is greatly acknowledged for supporting the postdoctoral study of M.G. at Virginia Commonwealth University. The authors appreciate the analytical help of Ms. Carmel Tebyanian (Chemical and Life Science Department, Virginia Commonwealth University).

■ REFERENCES

(1) Tans, P.; Keeling, R. *Trends in Atmospheric Carbon Dioxide*; http://www.esrl.noaa.gov/gmd/ccgg/trends/ (accessed August, 2015).

(2) Guido, Z. *Past and Present Climate*; http://www.southwestclimatechange.org/climate/global/past-present (accessed August 2015).

(3) Metz, B.; Davidson, O.; Coninck, H. D.; Loos, M.; Meyer, L. *IPCC Special Report on Carbon Dioxide Capture and Storage*; Cambridge University Press: New York, 2005.

(4) Khoo, H. H.; Bu, J.; Wong, R. L.; Kuan, S. Y.; Sharratt, P. N. Carbon capture and utilization: Preliminary life cycle CO_2, energy, and cost results of potential mineral carbonation. *Energy Procedia* **2011**, *4*, 2494−2501.

(5) Zevenhoven, R.; Fagerlund, J.; Nduagu, E.; Romão, I.; Jie, B.; Highfield, J. Carbon Storage by Mineralisation (CSM): Serpentinite Rock Carbonation via $Mg(OH)_2$ Reaction Intermediate Without CO_2 Pre-separation. *Energy Procedia* **2013**, *37*, 5945−5954.

(6) Seifritz, W. CO_2 disposal by means of silicates. *Nature* **1990**, *345*, 486.

(7) Zhao, H.; Park, Y.; Lee, D. H.; Park, A.-H. A. Tuning the dissolution kinetics of wollastonite via chelating agents for CO_2 sequestration with integrated synthesis of precipitated calcium carbonates. *Phys. Chem. Chem. Phys.* **2013**, *15* (36), 15185−15192.

(8) Sun, Y.; Parikh, V.; Zhang, L. Sequestration of carbon dioxide by indirect mineralization using Victorian brown coal fly ash. *J. Hazard. Mater.* **2012**, *209−210*, 458−466.

(9) Rahmani, O.; Junin, R.; Tyrer, M.; Mohsin, R. Mineral Carbonation of Red Gypsum for CO_2 Sequestration. *Energy Fuels* **2014**, *28* (9), 5953−5958.

(10) Zevenhoven, R.; Fagerlund, J., 16-Mineralisation of carbon dioxide (CO_2). In *Developments and Innovation in Carbon Dioxide (CO_2) Capture and Storage Technology*; Maroto-Valer, M. M., Ed.; Woodhead Publishing: Cambridge, U. K., 2010; Vol. 2, pp 433−462.

(11) Swanson, E. J.; Fricker, K. J.; Sun, M.; Park, A.-H. A. Directed precipitation of hydrated and anhydrous magnesium carbonates for carbon storage. *Phys. Chem. Chem. Phys.* **2014**, *16* (42), 23440−23450.

(12) Krevor, S. C.; Lackner, K. S. Enhancing process kinetics for mineral carbon sequestration. *Energy Procedia* **2009**, *1* (1), 4867−4871.

(13) Lako, P.; van der Welle, A. J.; Harmelink, M.; van der Kuip, M. D. C.; Haan-Kamminga, A.; Blank, F.; De Wolff, J.; Nepveu, M. Issues concerning the implementation of the CCS directive in the Netherlands. *Energy Procedia* **2011**, *4*, 5479−5486.

(14) Kainiemi, L.; Eloneva, S.; Toikka, A.; Levänen, J.; Järvinen, M. Opportunities and obstacles for CO_2 mineralization: CO_2 mineralization specific frames in the interviews of Finnish carbon capture and storage (CCS) experts. *J. Cleaner Prod.* **2015**, *94*, 352−358.

(15) Roskill, I. S. *Boron: Global Industry Markets and Outlook*, Twelfth ed.; Roskill Information Services Limited: London, 2010.

(16) Bulutcu, A. N.; Ertekin, C. O.; Celikoyan, M. B. K. Impurity control in the production of boric acid from colemanite in the presence of propionic acid. *Chem. Eng. Process.* **2008**, *47* (12), 2270−2274.

(17) Nelson, N. P. *Production of Boric Acid*; April 24, 1962.

(18) Gülensoy, H.; Kocakerim, M. M. Solubility of Colemanite Mineral in CO_2 -Containing Water and Geological Formation of This Mineral. *Bull. Miner. Res. Explor. Inst. Turk.* **1978**, *90*, 1−19.

(19) Yilmaz, O.; Unlu, F.; Karakoc, G.; Marasliogl u, D.; Gokcek, S.; Karacay, E.; Demirhan, M. H.; Cetin, C. E.; Iplikcioglu, O. *Production of Boric Carbonate and Sodium Bicarbonate from Sodium Borate Solvents*. Patent WO2010140989 A1, 2010.

(20) Ata, O. N.; ÇOlak, S.; Çopur, M.; Çelik, C. Determination of the Optimum Conditions for Boric Acid Extraction with Carbon Dioxide Gas in Aqueous Media from Colemanite Containing Arsenic. *Ind. Eng. Chem. Res.* **2000**, *39* (2), 488−493.

(21) Budak, A.; Gönen, M. Extraction of boric acid from colemanite mineral by supercritical carbon dioxide. *J. Supercrit. Fluids* **2014**, *92*, 183−189.

(22) Guo, H.; Chen, Y.; Hu, Q.; Lu, W.; Ou, W.; Geng, L. Quantitative Raman spectroscopic investigation of geo-fluids high-pressure phase equilibria: Part I. Accurate calibration and determination of CO_2 solubility in water from 273.15 to 573.15 K and from 10 to 120 MPa. *Fluid Phase Equilib.* **2014**, *382*, 70−79.

(23) Peng, C.; Crawshaw, J. P.; Maitland, G. C.; Martin Trusler, J. P.; Vega-Maza, D. The pH of CO_2-saturated water at temperatures between 308 and 423 K at pressures up to 15 MPa. *J. Supercrit. Fluids* **2013**, *82*, 129−137.

(24) Hagenson, L. C. *Sonochemical reactions: mass transfer and kinetic studies of a solid-liquid system*. Ph.D. Thesis, Iowa State University, Ames, IA, 1997.

(25) Okur, H.; Tekin, T.; Ozer, A. K.; Bayramoglu, M. Effect of ultrasound on the dissolution of colemanite in H_2SO_4. *Hydrometallurgy* **2002**, *67* (1−3), 79−86.

(26) Hollander, M.; Rieman, W., III Titration of Boric Acid in Presence of Mannitol. *Ind. Eng. Chem., Anal. Ed.* **1945**, *17* (9), 602−603.

(27) Marr, R.; Gamse, T. Use of supercritical fluids for different processes including new developments—a review. *Chem. Eng. Process.* **2000**, *39* (1), 19−28.

(28) Patnaik, P. *Handbook of Inorganic Chemicals*; Mc. Graw-Hill Handbooks: New York, 2002; p 1086.

(29) Taylan, N.; Gürbüz, H.; Bulutcu, A. N. Effects of ultrasound on the reaction step of boric acid production process from colemanite. *Ultrason. Sonochem.* **2007**, *14* (5), 633−638.

(30) Colthup, N. B.; Daly, L. H.; Wiberley, S. E. *Introduction to Infrared and Raman Spectrsocopy*, Third ed.; Academic Press. Inc.: San Diego, 1990; p 547.

(31) Jun, L.; Shuping, X.; Shiyang, G. FT-IR and Raman spectroscopic study of hydrated borates. *Spectrochim. Acta, Part A* **1995**, *51* (4), 519−532.

(32) Sanders, J. P.; Gallagher, P. K. Kinetic analyses using simultaneous TG/DSC measurements: Part I: decomposition of

DOI: 10.1021/acs.iecr.6b00378
Ind. Eng. Chem. Res. 2016, 55, 5116−5124

calcium carbonate in argon. *Thermochim. Acta* **2002**, *388* (1−2), 115−128.
(33) Levenspiel, O. *Chemical Reaction Engineering*; Wiley: New York, 1972.
(34) Hagenson, L. C.; Doraiswamy, L. K. Comparison of the effects of ultrasound and mechanical agitation on a reacting solid-liquid system. *Chem. Eng. Sci.* **1998**, *53* (1), 131−148.
(35) Kuskay, B.; Bulutcu, A. N. Design parameters of boric acid production process from colemanite ore in the presence of propionic acid. *Chem. Eng. Process.* **2011**, *50* (4), 377−383.

DOI: 10.1021/acs.iecr.6b00378
Ind. Eng. Chem. Res. 2016, 55, 5116−5124